nature cell biology

Transcriptional repression of p53 by parkin and impairment by mutations associated with autosomal recessive juvenile Parkinson's disease

Cristine Alves da Costa[1,8], Claire Sunyach[1], Emilie Giaime[1], Andrew West[2], Olga Corti[3], Alexis Brice[3], Stephen Safe[4], Patrick M. Abou-Sleiman[5], Nicholas W. Wood[5], Hitoshi Takahashi[6], Mathew S. Goldberg[7], Jie Shen[7] and Frédéric Checler[1,8]

Mutations of the ubiquitin ligase parkin account for most autosomal recessive forms of juvenile Parkinson's disease (AR-JP). Several studies have suggested that parkin possesses DNA-binding and transcriptional activity. We report here that parkin is a p53 transcriptional repressor. First, parkin prevented 6-hydroxydopamine-induced caspase-3 activation in a p53-dependent manner. Concomitantly, parkin reduced p53 expression and activity, an effect abrogated by familial parkin mutations known to either abolish or preserve its ligase activity. ChIP experiments indicate that overexpressed and endogenous parkin interact physically with the *p53* promoter and that pathogenic mutations abolish DNA binding to and promoter transactivation of p53. Parkin lowered *p53* mRNA levels and repressed *p53* promoter transactivation through its Ring1 domain. Conversely, parkin depletion enhanced p53 expression and mRNA levels in fibroblasts and mouse brains, and increased cellular p53 activity and promoter transactivation in cells. Finally, familial parkin missense and deletion mutations enhanced p53 expression in human brains affected by AR-JP. This study reveals a ubiquitin ligase-independent function of parkin in the control of transcription and a functional link between parkin and p53 that is altered by AR-JP mutations.

Parkinson's disease is a movement disorder characterized by severe loss of dopaminergic neurons, probably through apoptosis. This syndrome is mainly idiopathic but about 5% of cases are linked to a Mendelian pattern of inheritance and may be associated with an autosomal dominant or recessive mode of transmission. Parkin is associated with autosomal recessive juvenile forms of Parkinson's disease[1] and has been characterized as a ubiquitin ligase[2] that acts as a negative modulator of apoptosis, both *in vitro* and *in vivo*[3,4]. Enzymatic activity of parkin is abolished by several mutations associated with AR-JP. This functional deficit, therefore, has been proposed as a mechanism for the accumulation of proteasome-resistant, and potentially toxic, proteins observed in parkin-related familial cases of AR-JP[2].

Interestingly, several lines of evidence indicate that parkin could also behave as a transcription factor. First, parkin has been shown to be localized in the nucleus[5,6], a feature confirmed by our immunohistochemical analysis of parkin expression in human cells (Supplementary Information, Fig. S1). Second, parkin harbours a Ring-IBR-Ring domain, which predicts putative DNA binding and transcriptional activity properties[7]. Third, parkin downregulates expression of genes that encode various proteins, the levels of which are enhanced by apoptotic stimuli[8]. Thus, parkin was found to prevent ceramide-induced upregulation of various genes, including *CHK*, *EIF4EBP1*, *GADD45A* and *PTPN-5* (ref. 8). However, whether the cytoprotective effect of parkin was associated with its ability to control proteasomal degradation and cellular homeostasis of a set of cell death modulators through its ubiquitin ligase activity or whether this phenotype was linked to a direct or indirect modulation of gene expression remains questionable. Notably, putative target genes under direct parkin-mediated transcriptional control have not yet been documented. Here, we demonstrate that parkin acts as a transcriptional repressor of p53 independently of its ubiquitin ligase function and that parkin mutations associated with familial AR-JP abolish the parkin-mediated control of p53, both *in vitro* and *in vivo*. Furthermore, mapping of the parkin domain involved in p53 transcriptional regulation indicates an essential role of the Ring1 parkin domain, confirming the importance of the carboxy-terminal R1-IBR-R2 motif identified by empirical sequence-database searches[7].

[1]Institut de Pharmacologie Moléculaire et Cellulaire and Institut de NeuroMédecine Moléculaire, UMR6097 CNRS/UNSA, Équipe labellisée Fondation pour la Recherche Médicale, 660 Route des Lucioles, 06560, Valbonne, France. [2]Institute for Cell Engineering, Johns Hopkins University School of Medicine, Baltimore, MD 21287, USA. [3]INSERM U679, Hôpital de la Pitié-Salpêtrière, 47 boulevard de l'Hôpital, 75013 Paris, France. [4]Center for Environmental & Genetic Medicine, Institute of Biosciences & Technology, Houston, USA. [5]Department of Molecular Neuroscience, Institute of Neurology, Queen Square, London WC1N 3BG, UK. [6]Brain Research Institute, University of Niigata, 1-757 Asahimachi, Niigata 951-8585, Japan. [7]Center of Neurological Diseases, Harvard Medical School, Boston, Massachusetts, USA.
[8]Correspondence should be addressed to C.A.d.C. or F. C. (e-mail: acosta@ipmc.cnrs.fr; checler@ipmc.cnrs.fr)

Received 20 March 2009; accepted 14 July 2009; published online 4 October 2009; DOI: 10.1038/ncb1981

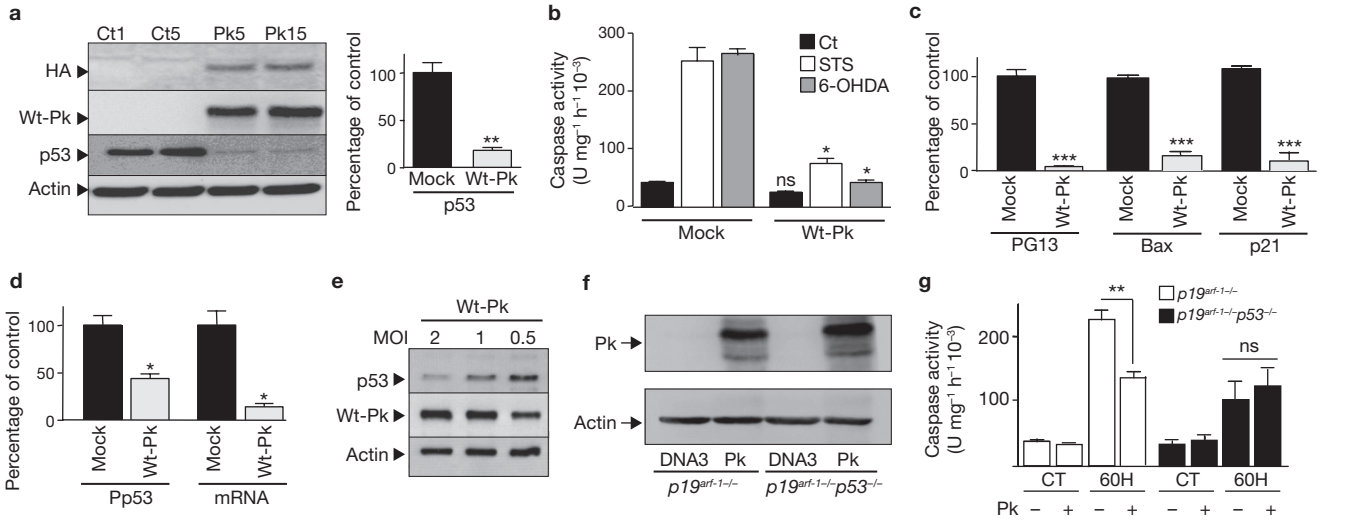

Figure 1 Protective effect of parkin is associated with modulation of p53 in TSM1 neuronal cell line. (**a**) Analysis of endogenous (Wt-Pk) and HA-tagged-parkin (HA), p53 and actin-like immunoreactivity in stably transfected TSM1 cells overexpressing either wild-type parkin (Pk) or empty vector (Ct) (numbers indicate distinct clones). The right panel shows the densitometric analysis of p53-like immunoreactivity (normalized to actin expression) expressed as percentage of control mock-transfected cells. Bars represent the mean ± s.e.m. of 3 independent experiments performed in duplicate (**$P < 0.001$). (**b**) Determination of caspase-3 activity in TSM1 neurons overexpressing empty vector (mock) and wild-type parkin (Wt-Pk) after treatment with staurosporine (STS, 1 μM) for 2 h or 6-hydroxydopamine (6OHDA, 0.2 mM) for 8 h. Bars represent the mean ± s.e.m. of 5 independent experiments performed in duplicate (*P <0.01 for Wt-Pk compare with Mock). (**c**, **d**) Analysis of p53 activity (PG13, Bax and p21), promoter transactivation (Pp53) and mRNA levels (mRNA) in Mock- and Wt-Pk-transfected cells (clone Pk15, see **a**). Values are normalized for transfection efficiency (β-galactosidase activity), expressed as percentage of mock-transfected cells (taken as 100) and are the mean ± s.e.m. of 4 (Pp53, mRNA and PG13) or 5 (Bax and p21) independent experiments performed in duplicate (*P <0.01, **P <0.001, ***P <0.0001). (**e**) p53 expression in lentiviral-infected primary cultured neurons overexpressing parkin. Primary cultured neurons were infected with 0.5, 1 and 2 MOI (multiplicity of infection) of Wt-Pk-lentiviral vector and then assayed for parkin and p53 expression four days after infection. (**f**, **g**) $p19^{arf-/-}$ and $p19^{arf-/-/p53-/-}$ fibroblasts were transiently transfected with empty pcDNA3 (DNA3) or *parkin* (Pk) cDNA. Twenty-four hours after transfection, cells were treated with 6-OHDA (6OH, 0.2 mM) for 8 h then expression of parkin (**f**) and caspase-3 activity (**g**) were monitored. Bars represent mean ± s.e.m. of 3 independent experiments performed in triplicate (**P <0.001; ns, not significant). Parkin and actin levels were assessed on separate gels as explained in Methods. Full scans of the blots in **a**, **e** and **f** are available in Supplementary Information, Fig.S3.

We have obtained stably transfected TSM1 neurons overexpressing HA-tagged wild-type parkin (Wt-Pk, Fig.1a). Determination of parkin immunoreactivity using antibodies directed against the HA tag and the native C terminus of parkin indicate a high enrichment of parkin expression when compared with its endogenous levels. Wt-Pk (clone 15, Fig. 1a and clone 5, data not shown) protects TSM1 neurons from a variety of pro-apoptotic stimuli. Thus, Wt-Pk reduced staurosporine- (STS) and 6-hydroxydopamine (6-OHDA)-induced caspase-3 activation by 70% and 84%, respectively (n = 10, P <0.01, compared with mock-treated cells; Fig. 1b). In addition to the parkin-associated protective phenotype, we have established that parkin controls the p53 pathway at several levels. Thus, overexpression of Wt-Pk induced marked reductions in p53 expression (p53, 82%, n = 6, P <0.001, Fig. 1a), transcriptional activity (PG13, Bax and p21, 96%, n = 6–10, P <0.0001, Fig.1c), promoter transactivation (Pp53, 56%, n = 6, P <0.01, Fig. 1d) and mRNA levels (mRNA, 86%, n = 3, P <0.01, Fig. 1d) when compared with mock-transfected control cells. Interestingly, increasing expression levels of Wt-Pk reduced p53 expression in a concentration-dependent manner in lentiviral-infected primary cultured neurons (Fig. 1e).

We examined whether parkin-associated reduction of 6-OHDA-stimulated caspase-3 activity was strictly dependent on p53 by comparing the effect of parkin overexpression (Fig.1f) in $p19^{Arf-1-/-}$ and $p19^{Arf-1-/-}p53^{-/-}$ fibroblasts. These two cell systems allow examination of the effect of p53 on apoptosis without the influence of this oncogene on cell cycle control[9]. Parkin reduced 6-OHDA-induced caspase-3 activation in $p19^{arf-1-/-}$ cells (Fig.1g). Clearly, although caspase-3 could be stimulated by 6-OHDA in $p19^{Arf-1-/-}p53^{-/-}$, p53 depletion fully prevented parkin-associated reduction of 6-OHDA-induced caspase-3 activation in this cell system (Fig. 1g). This finding indicates that control of 6-OHDA-stimulated caspase-3 activity by parkin was strictly p53-dependent, at least in fibroblasts.

To examine the implication of p53 control by endogenous parkin, we analysed the responsiveness of fibroblasts devoid of parkin (Pk^-) to 6-OHDA. Parkin depletion led to a substantial augmentation of caspase-3 activity under control (163%, n = 6, P <0.05) and 6-OHDA-induced conditions (247%, n = 6, P <0.01, Fig. 2a). Parkin depletion also increased p53 expression (231% of control, n = 6, P <0.01, Fig. 2b), activity (PG13, 632%, n = 6, P <0.01, Fig. 2c), promoter transactivation (Pp53, 275%, n = 6, P <0.01, Fig. 2c) and mRNA levels (338%, n = 5, P <0.05, Fig. 2c). Of particular interest, we established that brain homogenates prepared from *parkin* knockout mice also showed increased p53 expression (145% of wild-type brain, n = 4, P <0.05, Fig. 2d) and mRNA levels (224% of wild-type brain, n = 4, P <0.05, Fig. 2e). Thus, our data demonstrate that endogenous parkin down-regulates the p53 pathway both *in vitro* and *in vivo*.

We examined whether parkin mutations associated with AR-JP (Supplementary Information, Table S1) could impair the protective phenotype elicited by wild-type parkin. To determine whether a putative loss of parkin function correlates with abrogation of its ligase activity, we examined the influence of various familial mutations known to either abolish (C418R and C441R) or preserve (K161N and R256C) this catalytic activity. We transiently transfected wild-type parkin or its mutants in SH-SY5Y

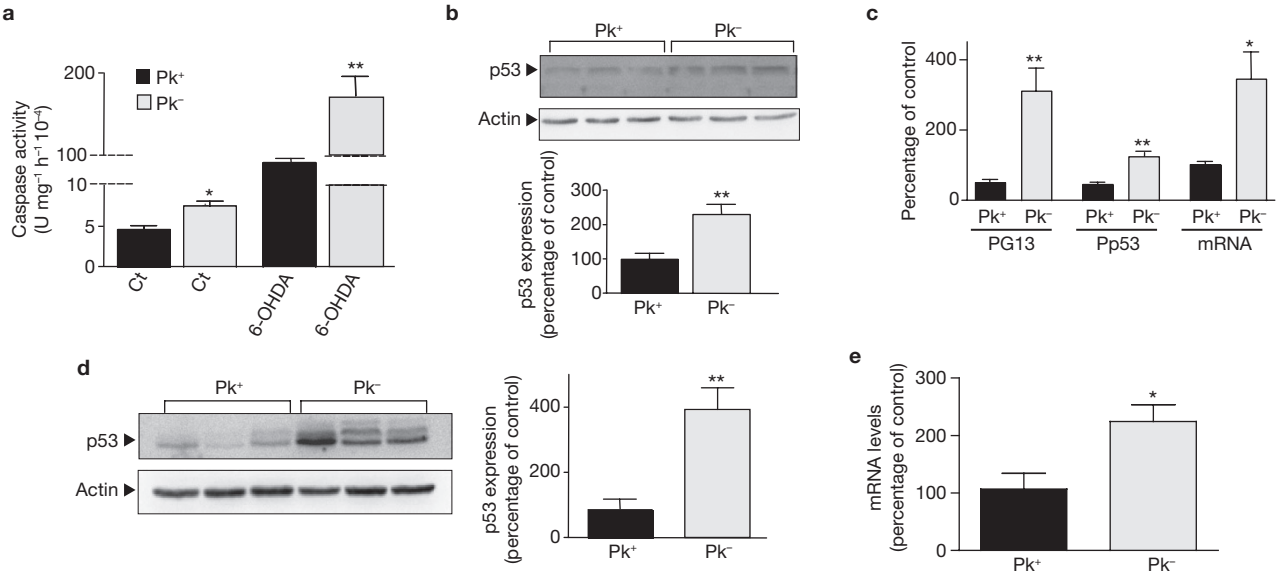

Figure 2 p53 pathway is upregulated in parkin-deficient fibroblasts and mouse brains. (**a**) Caspase-3 activity in 6-OHDA-treated (0.2 mM, 8 h) wild-type (Pk^+) and parkin-deficient (Pk^-) fibroblasts. Bars represent the mean ± s.e.m. of 3 independent experiments performed in triplicate (*P <0.05; **P <0.01). (**b**) p53 and actin expression in Pk^+ and Pk^- fibroblasts were determined by western blotting. The lower panel shows densitometric analysis of p53 (normalized by actin expression) and bars represent mean ± s.e.m. of 3 independent experiments performed in duplicate (**P <0.01). (**c**) Analysis of p53 activity (PG13), promoter transactivation (Pp53) and mRNA levels in *Pk*$^+$ and *Pk*$^-$ fibroblasts. Values normalized for transfection efficiency (β-galactosidase activity) are expressed as percentage of mock-transfected cells (taken as 100). Bars represent the mean ± s.e.m. of 3 independent experiments performed in duplicate (*P <0.05; **P <0.01). (**d**) p53 and actin immunoreactivity in brain homogenates derived from Pk^+ and Pk^- mice were determined. The right panel shows densitometric analysis of p53 (normalized by actin levels) and bars represent the mean ± s.e.m. of 5 brains analysed in duplicate (**P <0.01). (**e**) Densitometric analysis of *p53* mRNA levels derived from Pk^+ and Pk^- mice measured by RT–PCR. Bars represent the mean ± s.e.m. of 4 brains analysed in duplicate (*P <0.05). Full scans of the blots in **b** and **d** are available in Supplementary Information, Fig.S3.

cells and measured caspase-3 activity. With respect to Parkinson's disease pathology, it is interesting to note first that wild-type parkin protected the dopaminergic neuroblastoma cell line SH-SY5Y from caspase-3 activation triggered by 6-OHDA (Fig. 3a), a natural dopaminergic toxin frequently used to trigger phenotypes resembling Parkinson's disease *in vivo*[10]. Thus, wild-type parkin significantly decreased caspase-3 activity (43% of reduction, $n = 6$, P <0.05, Fig. 3a), p53 expression (Fig. 3b) and p53 promoter activity ($n = 6$, P <0.05, Fig. 3c) in 6-OHDA-treated SH-SY5Y cells. We note that expression of mutant parkin varied slightly in our transfection experiments (Fig. 3b). This variation could not be attributed to differences in transfection efficiencies, as neomycin phosphotransferase II expression was similar (Fig. 3b). A more likely explanation is the distinct catabolic susceptibilities of parkin mutants as previously reported[11]. However, this slight variation in catabolic fate is probably cell-specific (see similar expressions after transfection in fibroblasts in Fig. 3d) and does not influence the phenotype triggered by all parkin mutations. Thus, neither ligase-active nor ligase-dead mutants were able to affect 6-OHDA-stimulated caspase-3 activity (Fig. 3a), and increased both p53 expression (Fig. 3b) and promoter transactivation (Fig. 3c). Another mutation (R42P) also abolished parkin-induced reduction of p53 in lentiviral-infected primary cultured neurons (data not shown).

We examined the potential of wild-type and mutated parkin to restore the parkin-associated phenotype in parkin-deficient fibroblasts. First we established that wild-type parkin lowers *p53* promoter transactivation in wild-type fibroblasts (35% of reduction, $n = 6$, P <0.05, data not shown). Transient transfection of wild-type *parkin* cDNA in parkin-deficient fibroblasts lowered p53 expression (Fig. 3d), promoter transactivation (Fig. 3e) and mRNA levels (Fig. 3f). This phenotype was not observed with parkin mutants (Fig. 3d–f). These data clearly establish that parkin-associated downregulation of p53 transcription is abolished by familial Parkinson's disease mutations independently of its ubiquitin ligase activity and is consistent with our experiments failing to demonstrate a parkin-mediated ubiquitylation of p53 (data not shown).

To our knowledge, only six human brain samples are available worldwide (Supplementary Information, Table S1) to examine whether patients with Parkinson's disease carrying a parkin mutation show any alteration in their endogenous content of p53. We were able to obtain two brain samples carrying either a point mutation or an exon deletion (see Methods). Although the number of pathological samples was small, we observed a reproducible and consistent increase in p53-like immunoreactivity in AR-JP brains (454% of control brains, $n = 2$, Fig. 3g) and we established that brain sample harbouring the exon 4 deletion (Supplementary Information, Table S1) shows higher *p53* mRNA levels (data not shown). These data suggest that the ability of parkin mutations to downregulate the p53 pathway in cells could indeed reflect alterations occurring in pathological brains.

One of the main cell survival molecular pathways involves phosphorylation of Akt/PKB mediated by phosphatidylinositol-3-kinase[12]. Several studies have consistently documented a molecular cascade linking Akt and NFκB that ultimately leads to p53 inhibition and cell survival[13]. It was of interest therefore to examine whether the selective Akt inhibitor LY294002 could prevent parkin-associated reduction of p53 pathway. Our data indicate that LY294002 did not modulate parkin-mediated reduction of 6-OHDA-stimulated caspase-3 activity (Supplementary Information, Fig. S2), suggesting that the control of p53 by parkin occurs mainly at the transcriptional level.

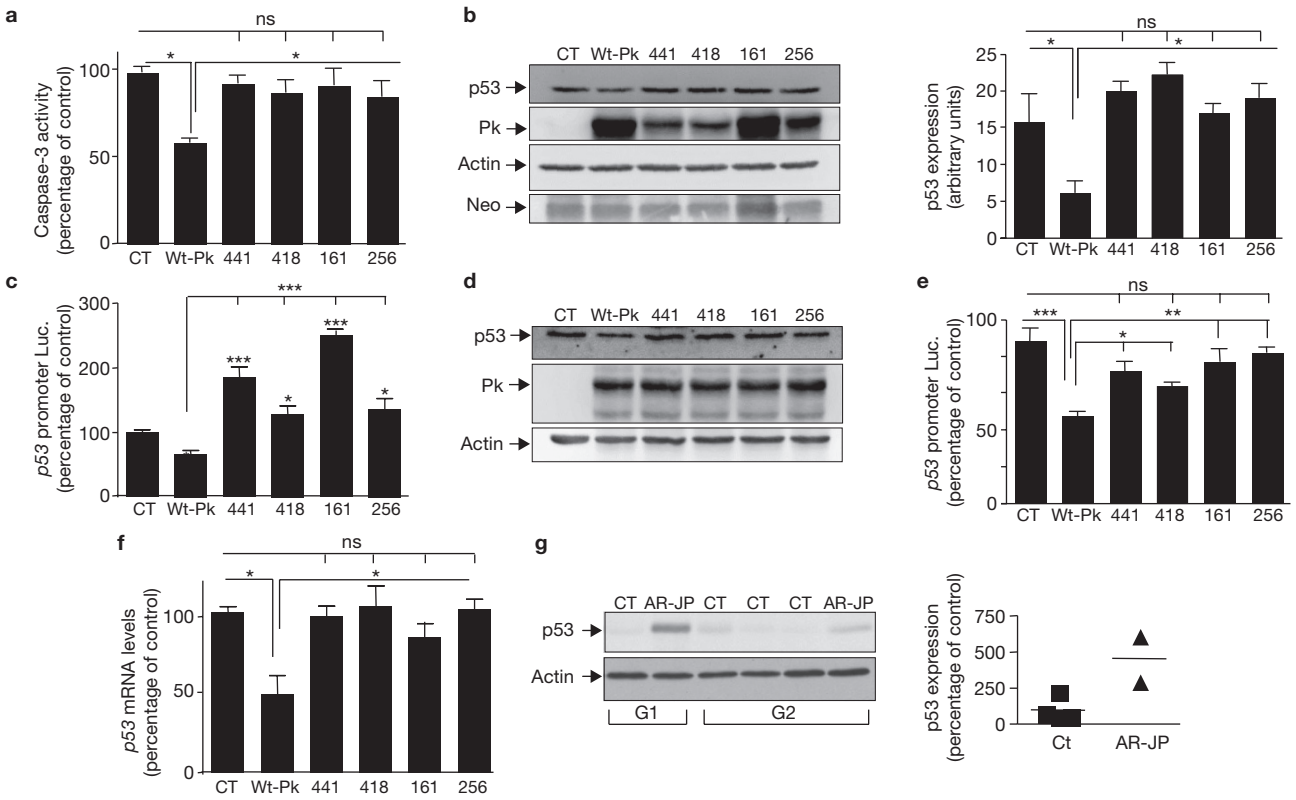

Figure 3 Mutations associated with familial Parkinson's disease abolish the ability of parkin to control p53 and do not rescue parkin function in parkin-deficient fibroblasts. (**a**–**c**) Caspase-3 activity (**a**), p53 and parkin expression (**b**) and *p53* promoter transactivation (**c**) in SH-SY5Y cells transiently transfected with empty vector (CT), wild-type parkin (Wt-Pk) and the C418R (418), C441R (441), K161N (161) and R256C (256) mutated parkin constructs. Actin and neomycin phosphotransferase II (Neo) expression (**b**, left panel) were determined to control transfection efficiency and protein loading. p53 expression (**b**, right panel) was normalized by actin immunoreactivity. The transfection efficiencies were normalized after co-transfection of β-galactosidase cDNA. Values are expressed as percentage of mock-transfected SH-SY5Y cells (controls taken as 100) and are the mean ± s.e.m. of 3 independent experiments performed in triplicate (*P <0.05, ***P <0.001, ns, not statistically significant). (**d**–**f**) p53 expression (**d**), promoter transactivation (**e**) and mRNA levels (**f**) in parkin-deficient cells transiently transfected with empty vector (CT), wild-type parkin (Wt-Pk) and the C418R (418), C441R (441), K161N (161) and R256C (256) mutated parkin constructs. Values are expressed as percentage of mock-transfected parkin-deficient fibroblasts (controls taken as 100) and are the mean ± s.e.m. of 3 independent experiments performed in triplicate (*P <0.05, **P <0.01, ***P <0.001, ns, not statistically significant). (**g**) Parkin mutations increase p53 expression in AR-JP-affected human brains. p53 expression and densitometric analyses in control (CT) and pathological (familial Parkinson's disease, AR-JP) human brains (group 1 (G1) represents the 'England' samples and group 2 (G2) the 'Japan' samples). Parkin and actin levels were assessed on separate gels as explained in Methods. Full scans of the blots in **b**, **d** and **g** are available in Supplementary Information, Fig.S3.

We have delineated the p53 domain with which parkin could functionally interact by means of deletion analysis of the 5′ *p53* promoter region. Parkin-induced reduction of luciferase activity was abolished when the -312 to -196 sequence was deleted (compare p53-4 and p53-5 constructs; Fig. 4a, b). Accordingly, we examined whether parkin could physically interact with this *p53* promoter region. We designed three probes covering the -312 to -130 promoter sequence of *p53* (Fig. 4c). Our data show that parkin interacts only with the -312 to -243 promoter region covered by Pp53-A probe (Fig. 4d, left panel), whereas parkin did not interact with the Pp53-B and Pp53-C probes (Fig. 4d). Importantly, parkin-Pp53-A interaction was observed for both endogenous and overexpressed parkin in HEK human 293 cells (Fig. 4d, right panel), as can be deduced from increased labelling of the parkin–Pp53-A complex observed in cells overexpressing parkin. The specificity of the interaction was further supported by super-shift experiments that indicate downregulation of the parkin–Pp53-A complex in the presence of a specific antibody directed towards parkin, as well as by the full displacement of the parkin–Pp53-A labelling by a 20-fold excess of cold-specific (cs) Pp53-A probe (Fig. 4d, right panel). To definitively establish that endogenous parkin physically interacted with the *p53* promoter, we carried out chromatin immunoprecipitation (ChIP) experiments using a set of primers encompassing the p53 promoter region mapped in Fig. 4b, d. We confirmed that endogenous parkin indeed binds to the mouse *p53* promoter (Fig. 4e, see lane IP in Pk^+). Specificity of this interaction was demonstrated by the lack of PCR amplification product detectable after ChIP analysis in parkin-deficient fibroblasts (Fig. 4e, compare lanes IP in Pk^+ and Pk^-). ChIP analyses also showed that all parkin mutations examined here markedly reduced parkin binding to the *p53* promoter (Fig. 4f, compare IP lanes).

Finally, we delineated the parkin domain involved in p53 transcriptional repression. We focused on the Ring1-IBR-Ring2 domain harboured by parkin (Fig. 5a) for several reasons. First, the Ring1-IBR-Ring2 architectural feature has been identified as a consensus sequence found in a variety of important proteins with suspected transcription factor activities[7]. Second, the Ring1–IBR–Ring2 sequence of RBCK1 alone was found to be sufficient to induce transcription of a reporter gene[14]. Transient co-transfection of cDNA encoding parkin domains encompassing Ring1/2 and/or IBR domains (Fig. 5a) together with the *p53* human promoter construct indicate that only the constructs

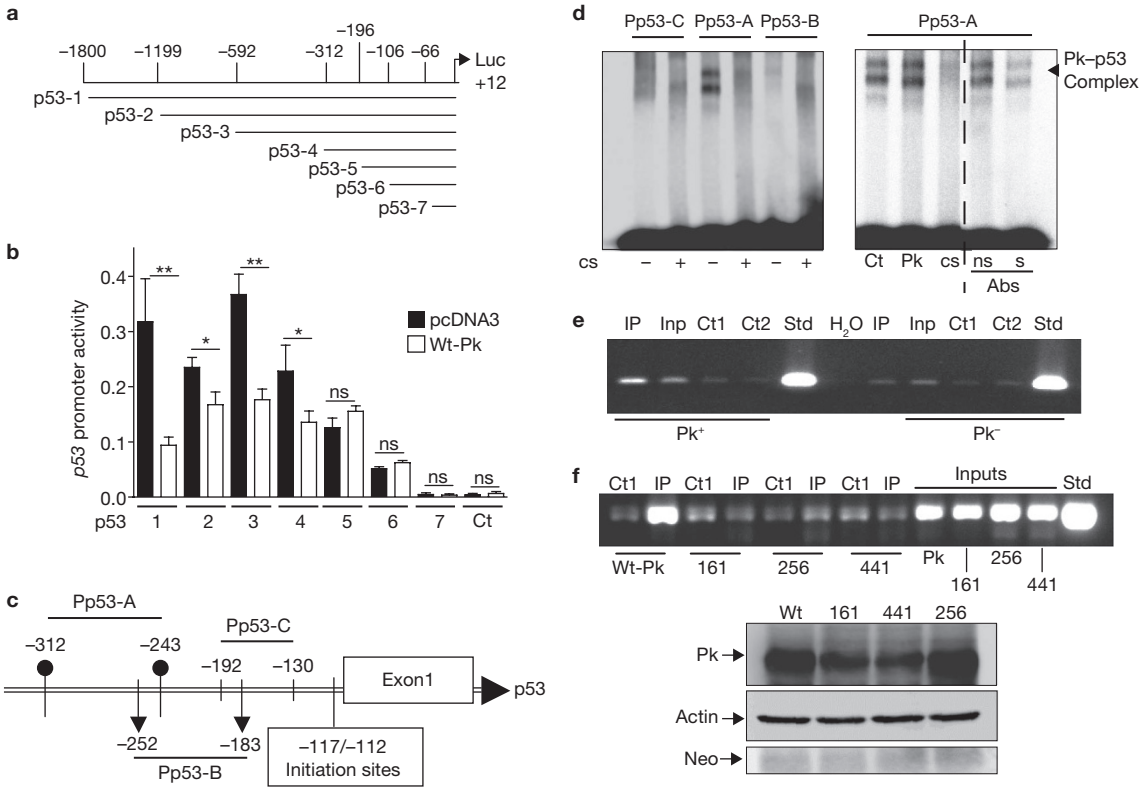

Figure 4 Deletion analysis of *p53* promoter transactivation by parkin and physical interaction between parkin and p53 promoter. (**a**) Representation of the 5′ deletion constructs (p53-n) of *p53* promoter region. (**b**) *p53* promoter transactivation in SH-SY5Y cells. The indicated *p53* promoter-luciferase constructs were co-transfected with the β-galactosidase reporter gene and either empty cDNA or wild-type *parkin* (Wt-Pk) cDNA. Bars represent the mean ± s.e.m. of 3 independent experiments performed in duplicate (**P* <0.05; ***P* <0.001). (**c**) Representation of human *p53* promoter regions covered by p53 probes (Pp53-A, Pp53-B and Pp53-C). (**d**) Gel retardation of nuclear preparations of HEK293 cells over-expressing Wt-Pk incubated with indicated labelled p53 probes with (–) or without (+) excess of cold p53 probe (cs, cold-specific). Only Pp53-A reveals a specific and displaceable Pk–p53 complex. Gel retardation of nuclear preparations of HEK293 cells transiently transfected with empty vector (Ct) or HA-tagged Wt-Pk (Pk) incubated with labelled Pp53-A probe (right, lanes 1,2); lanes 3, 4 and 5 correspond to lane 2 conditions with an excess of cold-specific Pp53-A probe, non-specific (ns, anti-V5) or specific (s, anti-Pk) competing antibodies (Abs), respectively. Pk–p53 complex is abolished only with cold-specific probe and specific antibody. Dotted line in **d**, right panel, indicates a lane that was removed (Supplementary Information, Fig. S3). (**e**, **f**) Interaction of parkin with mouse *p53* promoter by ChIP experiments in wild-type (Pk$^+$) and parkin-deficient (Pk$^-$) fibroblasts (**e**) or HEK293 cells transfected with wild-type parkin (Wt-Pk or Pk), K161N (161), R256C (256) and C441R (441) mutated parkin constructs. Agarose gels represent PCR products obtained with the mouse PCR primers covering the -330/-117 region mouse *p53* promoter (**e**) or the -533/-213 region of the human *p53* promoter (**f**). IP represent immunoprecipitations with specific parkin antibodies (MAB5512); Inputs (Inp) represent the DNA inputs in the indicated cells (**e**) or transfection conditions (**f**). Ct1 and Ct2 represent ChIP with non-correlated antibodies (IgG control) or RNA pol IgG, respectively. Std represents PCR products of mouse (**e**) or human (**f**) *p53* promoter constructs. Lower panel **f** describes parkin, actin and neomycin phosphotransferase II (Neo). Parkin and actin levels were assessed on separate gels as explained in Methods. For full scans of blots in **d**, **e** and **f** , see Supplementary Information, Fig. S3.

containing the Ring1 domain are able to downregulate *p53* promoter transcription in SH-SY5Y cells (Fig. 5b). Thus, full-length parkin and its Ring1 and Ring1–IBR-derived domains decreased *p53* promoter activity by approximately 40% when compared with empty vector transfected cells ($n = 9$, *P <0.05, **P < 0.01, Fig. 5b), whereas Ring2 and IBR–Ring2 expression remain biologically inert (Fig. 5b). These data clearly indicate that the Ring1 domain of parkin probably accounts for the ability of parkin to repress p53 transcription.

Interestingly, several ubiquitin ligases have been implicated in the post-translational control of p53 (refs 15–18). Among these ligases, MDM2, the major regulator of p53, binds to p53 and triggers 26S proteasome-mediated degradation and functional inactivation of p53 (ref. 19). Furthermore, MDM2 indirectly controls transcription of p53 through interaction with Nedd8 (ref. 20). However, our data have established that parkin-mediated control of p53 remains independent of its ubiquitin ligase activity.

All parkin mutations associated with familial cases of Parkinson's disease examined in this study markedly lowered both parkin binding to the *p53* promoter and *p53* promoter transactivation. Furthermore, although human brain samples were difficult to obtain, our set of anatomical pieces confirmed that p53 was abnormally high in parkin-associated familial Parkinson's disease brains. Several cases of AR-JP are linked to missense point mutations taking place in the Ring1 domain of parkin only[21]. However, our data show that mutations inside (R256C) and outside the Ring1 domain (C418R and C441R mutations are located in the Ring2 domain) similarly affect the parkin-associated control of p53 transcription. This suggests that all mutations located within the Ring1–IBR–Ring2 sequence arrangement alter the functionality of parkin by affecting the cooperativity of this functional tri-domain independently of any influence on parkin ubiquitin ligase activity. The finding that the K161N mutation located outside the Ring1–IBR–Ring2 also abolishes parkin-associated phenotype could suggest that additional

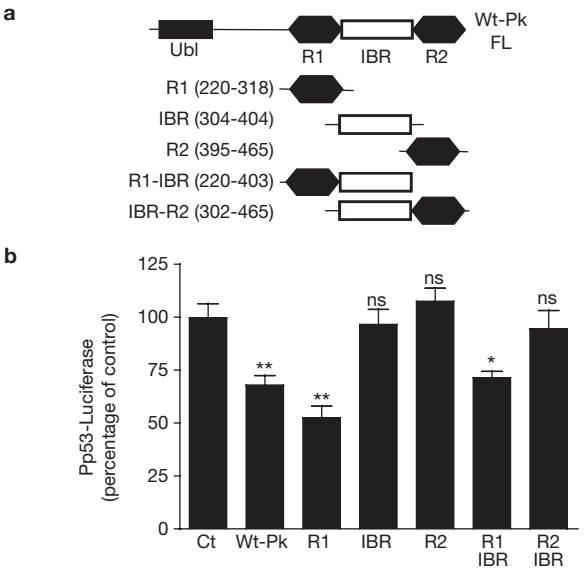

Figure 5 Mapping of the parkin domain involved p53 transcription repression. (**a**) Schematic representation of full-length (FL) and deleted parkin constructs. These constructs were co-transfected with the human *p53* promoter and β-galactosidase constructs (to normalize transfection efficiency) in SH-SY5Y neuroblastoma cells. (**b**) *p53* promoter transactivation in SH-SY5Y cells transiently transfected with empty vector (Ct), wild-type HA-parkin (Wt-Pk) and the indicated Myc-tagged parkin-deleted constructs. Values are expressed as percentage of empty-vector-transfected cells (controls taken as 100) and are the mean ± s.e.m. of 3 independent experiments performed in triplicate (*P <0.05,**P <0.01; ns, not statistically significant).

structural/conformational alterations could trigger the impairment of the interaction of the Ring1 domain of parkin with the p53 promoter. This agrees well with the observation that mutations located outside the Ring1–IBR–Ring2 domain responsible for ubiquitin ligase activity could also impair this activity through misfolding and destabilization of the protein[11].

Parkin is involved in the cellular homeastasis of a series of proteins by modulating their ubiquitylation and thereby controlling their subsequent degradation by the proteasome. Previous studies showed that familial parkin mutations could differently alter the biophysical properties and subcellular distribution of the protein but also affect its ubiquitin-dependent catalytic properties[22,23]. Our study delineates another function of parkin as a transcriptional repressor of p53, a function that could well be primarily responsible for the physiological control of the tumour repressor p53. It also shows that this function remains fully independent of parkin-associated ubiquitin ligase. As a corollary, it adds another level of complexity in the understanding of the molecular dysfunction accounting for the AR-JP cases related to mutations on this pleiotropic protein. □

METHODS

Methods and any associated references are available in the online version of the paper at http://www.nature.com/naturecellbiology/

Note: Supplementary Information is available on the Nature Cell Biology website.

ACKNOWLEDGEMENTS

We would like to thank Amanda Patel for helpful discussion concerning gel shift analyses. We wish to thank M. Oren, B. Vogelstein and T. Dawson for providing us with the *p53* promoter, PG13 and *parkin*-deleted constructs. M. Roussel and T. Dawson are thanked for providing the $p19^{Arf-1-/-}$ and $p19^{Arf-1-/-}p53^{-/-}$ and *parkin* knockout cells, and *parkin*-deletion constructs, respectively. We thank J. C. Bourdon for providing polyclonal p53-directed antibodies. We wish to thank F. Brau for help in confocal analysis and F. Aguila for artwork. This work was supported by the Fondation pour la Recherche Médicale.

AUTHORS CONTRIBUTIONS

S.C. and E.G. performed a subset of experiments and contributed equally to the work; A.W. performed lentiviral experiments; O.C. and A.B. provided *parkin* cDNA; N.W.W. and P.M.A.S. provided 'English' human brain samples; H.T. provided 'Japanese' human brain samples; M.S.G. and J.S. provided *parkin*-null fibroblasts and brains; S.S. provided p53 promoter constructs; C.A.C. and F.C. are co-senior contributors; C.A.C. designed the study, performed most of the experiments, discussed data and wrote the manuscript; F.C. discussed data and contributed to the writing of the manuscript.

COMPETING INTERESTS STATEMENT

The authors declare that they have no competing interests.

Published online at http://www.nature.com/naturecellbiology/
Reprints and permissions information is available online at http://npg.nature.com/reprintsandpermissions/

1. Kitada, T. *et al.* Mutations in the *parkin* gene cause autosomal recessive juvenile parkinsonism. *Nature* **392,** 605–608 (1998).
2. Shimura, H. *et al.* Familial Parkinson disease gene product, parkin, is a ubiquitin-protein ligase. *Nature Genet.* **25,** 302–305 (2000).
3. Jiang, H., Ren, Y., Zhao, J. & Feng, J. Parkin protects human dopaminergic neuroblastoma cells against dopamine-induced apoptosis. *Hum. Mol. Genet.* **13,** 1745–1754 (2004).
4. Pesah, Y. *et al. Drosophila* parkin mutants have decreased mass and cell size and increased sensitivity to oxygen radical stress. *Development* **131,** 2183–2194 (2004).
5. Cookson, M. R. *et al.* RING finger 1 mutations in Parkin produce altered localization of the protein. *Hum. Mol. Genet.* **12,** 2957–2965 (2003).
6. Horowitz, J. M., Myers, J., Vernace, V. A., Stachowiak, M. K. & Torres, G. Spatial distribution, cellular integration and stage development of Parkin protein in *Xenopus* brain. *Brain Res. Dev. Brain Res.* **126,** 31–41 (2001).
7. Morett, E. & Bork, P. A novel transactivation domain in parkin. *Trends in Biochem. Sci.* **24,** 229–231 (1999).
8. Unschuld, P. G. *et al.* Parkin modulates gene expression in control and ceramide-treated PC12 cells. *Mol. Biol. Rep.* **33,** 13–32 (2006).
9. Kamijo, T. *et al.* Tumor suppression at the mouse INK4a locus mediated by the alternative reading frame product p19ARF. *Cell* **91,** 649–659 (1997).
10. Sauer, H. & Ortel, W. H. Progressive degeneration of nigrostriatal dopamine neurons following intrastriatal terminal lesions with 6-hydroxydopamine: a combined retrograde tracing and immunocytochemical study in the rat. *Neuroscience* **59,** 401–415 (1994).
11. Henn, I. H., Gostner, J. M., Lackner, P., Tatzelt, J. & Winklhofer, K. F. Pathogenic mutations inactivate parkin by distinct mechanisms. *J. Neurochem.* **92,** 114–122 (2005).
12. Datta, S. R., Brunet, A. & Greenberg, M. E. Cellular survival: a play in three Akts. *Genes Dev.* **13,** 2905–2927 (1999).
13. Jeong, S. J., Pise-Masison, C. A., Radonovich, M. F., Park, H. U. & Brady, J. N. Activated AKT regulates NF-κB activation, p53 inhibition and cell survival in HTLV-1-transformed cells. *Oncogene* **24,** 6719–6728 (2005).
14. Tatematsu, K. *et al.* Transcriptional activity of RBCK1 protein (RBCC protein interacting with PKC 1): requirement of RING-finger and B-Box motifs and regulation by protein kinases. *Biochem. Biophys. Res. Comm.* **247,** 392–396 (1998).
15. Grossman, S. R. *et al.* Polyubiquitination of p53 by a ubiquitin ligase activity of p300. *Science* **300,** 342–344 (2003).
16. Esser, C., Scheffner, M. & Hohfeld, J. The chaperone-associated ubiquitin ligase CHIP is able to target p53 for proteasomal degradation. *J. Biol. Chem.* **280,** 27443–27448 (2005).
17. Leng, R. P. *et al.* Pirh2, a p53-induced ubiquitin-protein ligase, promotes p53 degradation. *Cell* **112,** 779–791 (2003).
18. Dornan, D. *et al.* The ubiquitin ligase COP1 is a critical negative regulator of p53. *Nature* **429,** 86–92 (2004).
19. Haupt, Y., Maya, R., Kazaz, A. & Oren, M. Mdm2 promotes the rapid degradation of p53. *Nature* **387,** 296–299 (1997).
20. Xirodimas, D. P., Saville, M. K., Bourdon, J. C., Hay, R. T. & Lane, D. P. Mdm2-mediated NEDD8 conjugation of p53 inhibits its transcriptional activity. *Cell* **118,** 83–97 (2004).
21. Hattori, N. *et al.* Point mutations (Thr240Arg and Gln311Stop) [correction of Thr240Arg and Ala311Stop] in the *Parkin* gene. *Biochem. Biophys. Res. Comm.* **249,** 754–758 (1998).
22. Sriram, S. R. *et al.* Familial-associated mutations differentially disrupt the solubility, localization, binding and ubiquitination properties of parkin. *Hum. Mol. Genet.* **14,** 2571–2586 (2005).
23. Wang, C. *et al.* Alterations in the solubility and intracellular localization of parkin by several familial Parkinson's disease-linked point mutations. *J. Neurochem.* **93,** 422–431 (2005).

DOI: 10.1038/ncb1981

METHODS

Cell systems and constructs. *Pk*$^{+/+}$, *Pk*$^{-/-}$, *p19*$^{Arf-1-/-}$ and *p19*$^{Arf-1-/-}$*p53*$^{-/-}$ fibroblasts were obtained and cultured as described previously[9,24]. TSM1 neurons expressing empty vector or wild-type HA-tagged parkin were obtained after transfection (2 μg of each cDNA) using lipofectamine according to manufacturer's conditions (Invitrogen). HEK293 cells, TSM1 and SH-SY5Y cells were grown in 5% CO_2 in Dulbecco's modified Eagle's medium (DMEM) supplemented with 10% fetal calf serum containing penicillin (100 U ml^{-1}) and streptomycin (50 μg ml^{-1}). Parkin mutations are summarized in Supplementary Information, Table S1.

Caspase-3 activity measurements. Cells were grown in 6-well plates and incubated without or with staurosporine (1 μM) or 6-OHDA (0.2 mM) for 2–4 and 8 h, respectively. When indicated, cells were treated or not for 30 min with LY294002 (10 μM) before 6-OHDA treatment. Caspase-3-like enzymatic activity was measured fluorimetrically by means of a microtitre plate reader (Labsystems, Fisher Bioblock Scientific), as extensively detailed previously[25].

Western blot analyses. Proteins (50 μg) were separated on 12% SDS–PAGE gels and wet-transferred to Hybond-C (Amersham Life Science) membranes. Immunoblotting was performed using mouse and human monoclonal (PAB240 and PAB1801 both at 1:1,000 dilutions; Santa Cruz, Biotechnology) or polyclonal (CM1 provided by J.C. Bourdon, Cell transformation research group, Cancer Research Uk, Dundee, Scotland, UK) anti-p53 antibodies (1:2,000), mouse monoclonal anti-HA antibodies (1:1,000; Covance), mouse anti-parkin antibodies (MAB5512, 1:1,000; Chemicon) or mouse monoclonal anti-actin antibodies (1:5,000; Sigma). Neomycin phosphotransferase II was revealed with the mouse monoclonal 4B4D1 (1:500) from Abcam. Immunological complexes were revealed with anti-mouse IgG-coupled to peroxidase (1:5,000; Immunotech) antibodies, followed by electrochemoluminescence revelation (Roche). In mouse TSM1 neurons and in primary cultured neurons, p53 and actin were analysed on the same gel, whereas parkin immunoreactivity from same samples was analysed on a separate gel run in parallel as parkin and p53 show very close relative molecular mass (55 and 53K, respectively), and therefore virtually co-migrate on 12% SDS–PAGE gels. Parkin and actin were always run on parallel gels as anti-parkin antibodies label an additional band at 48K, which is close to actin (46K, see full scans of parkin western blots in Figs 1a, 1f, 3b, 3d and 4f in Supplementary Information, Fig. S3). When p53 was analysed in the human cell line SH-SY5Y, we used a polyclonal antibody that is much more sensitive for human p53 but gives rise to non-specific bands (see full scan in Supplementary Information, Fig. S3, b) that co-migrates with actin. Therefore, actin from same samples was analysed in a parallel gel. When neomycin and parkin expressions were analysed, neomycin was analysed on same gels after nitrocellulose cutting (as neomycin requires longer exposure).

p53 activity and promoter transactivation. The p53 transcriptional activity (PG13, p21 and Bax) and promoter transactivation were measured as described previously[25]. The 5′ deletion *p53* promoter and Myc-tagged parkin domain constructs have been described previously[26,27]. All activities were measured after co-transfection of 0.5–1 μg of the above cDNAs and 0.2–0.5 μg of β-galactosidase cDNA to normalize transfection efficiencies as described previously[28].

Human and murine brain tissues. Both sample groups correspond to the striatum (nucleus caudate/putamen). The 'England' group includes one control brain and one AR-JP brain (female, 83 years, heterozygous missense mutation Arg275Trp in exon 7, Supplementary Information, Table S1). The 'Japan' group includes three control brains from patients with no history of dementia or other neurological diseases, and one AR-JP brain (male, 70 years, homozygous exon 4 deletion, Supp. Table 1). *Parkin* knockout murine brains have been described recently[29].

RT–PCR analysis of p53 mRNAs in cells and mice brain. Total RNA from cells was extracted using the RNeasy kit following the instructions of the manufacturer (Qiagen), reverse transcribed (AMV-transcriptase, Promega) then subjected to real-time PCR as described previously[28].

Electrophoretic mobility shift assay (EMSA). EMSA was performed using a commercial DNA-binding-protein detection system (Promega). In brief, three pairs of oligonucleotides (Pp53A, B and C forward and reverse, see below) covering distinct regions of the human p53 promoter (see Fig. 4c) were synthesized by Eurogentec, annealed and end-labelled using ^{32}P-ATP (6000 Ci mmol^{-1}, ICN Biomedicals). For the preparation of nuclear extracts, HEK293 cells were cultured in 100-mm diameter dishes and transiently transfected with either empty or HA-tagged parkin cDNA vectors (12 μg), using lipofectamine. Forty-eight hours after transfection, cells were recovered and nuclear extracts were prepared according to the *Current Protocols in Molecular Biology*[30]. Binding reactions containing nuclear extracts (10 μg) were performed at 37°C using the p53 probes according to the manufacturer's conditions. The specificity of the reactions described above was verified by a supershift assay where a pre-incubation (37°C, 10 min) of nuclear extracts with either MAB5512 (specific) or anti-V5 (non-specific) antibodies was performed before addition of the labelled probe and re-incubation at 37°C for 20 min. Then, protein–DNA complexes were resolved by electrophoresis (3 h at 300 V) on native polyacrylamide gels (7%) in Tris 5 mM, pH8.3 buffer containing glycine (38 mM). Gels were dried and subjected to autoradiography on a BAS-1500 phosphorimager (Fujifilm).

Pp53-A forward: 5′-GGCACCAGGTCGGCGAGAATCCTGACTCTGCACCCTCCTCCC CAACTCCATTTCCTTTGCTTCCTCG GC-3′, Pp53-A reverse: 5′-GCCGGAGGAAGC AAAGGAAATGGAGTTGGGGAGGAGGGTGCAGAGTCAGGATTCTCGCCGACC TGGTGCC-3′, Pp53-B forward: 5'-TTCCTCCGGCAGGCGGATTACTTGCCCTTACT TGTCATGG CGACTGTCGACCTTTGTGCCAGGAGCCTCG-3′, Pp53-B reverse:

5′-CGAGGCTCCTGGCACAAAGCTGGACAGTCGCCATGACAAGTAAGGGC AAGAATCCGCCTGGGAGGAA-3′. Pp53-C forward: 5′GCCAGGAGCCTCGCAGG GGTTGATGGGATTG GGGTTTTCCCCTCCCATG GCTCAAGACTGGCGC3',

Pp53-C reverse: 5′-GCGCCAGTCTTGAGCACATGGGAGGGGAAAACCCCAATCC CATCAACCCCTGCGAGGCTCCTGGC-3′.

Chromatin immunoprecipitation assay (ChIP). ChIP assay was performed according to ChIP-IT kit instructions (Active Motif). Briefly, to prepare chromatin, wild-type and *parkin* knockout cells MEFs were seeded in three 150-mm dishes and allowed to reach 70–80% confluence. In the case of HEK293 cells, cells were transfected with 12 μg of pcDNA3 empty vector or containing the cDNAs of wild-type and mutated *parkin*. Cells were fixed with formaldehyde and recovered in phosphate buffered saline (PBS), crosslinked and processed for chromatin preparation according to the manufacturer's recommendations. DNA obtained was digested either with the shearing enzyme (MEFs) provided in the kit, as recommended by the supplier or by sonication (HEK293 cells), yielding chromatin fragments of about 200-500 bp in size. Each immunoprecipitation was performed on 50 μg of chromatin in the ChIP immunoprecipitation buffer supplied, with 2 μg of anti-parkin primary antibody (MAB5512, Chemicon International) or irrelevant antibodies (IgG or RNApol IgG) as negative controls. Immunocomplexes were incubated (1.5 h, 4°C) with 100 μl of a solution of protein G-Sepharose. After elution of the immune complexes, crosslinks were reversed and RNA digested using RNase (100 μg ml^{-1}). To eliminate proteins, proteinase K (100 μg ml^{-1}) was added and the samples were incubated for 2 h at 42°C. DNA was purified on columns provided in the kit and PCR amplifications were performed using primers specific for the -330/-117 bp region of the mouse *p53* promoter (forward 5′-CGACTTTTCACAAAGCG -3′; reverse 5′-GCTACAGAACTTTAGCCAGG-3′) (MEF cells) or using primers specific for the -533/-213bp region of the human p53 promoter (forward 5′-GGGAGAAAACGTTAGGGTGT -3′; reverse 5′-CCATGACAAGTAAGGGCAAG -3′) (HEK293 cells).

Parkin lentivirus generation and primary cultures of neurons. The open-reading frame of human parkin fused to eGFP was inserted into the cFUGW lentiviral expression plasmid (a gift from David Baltimore, California Institute of Technology). Lentivirus was prepared as previously described[31]. Packaging constructs pLP1, pLP2 and pVSV-G (Invitrogen) were substituted into the production protocol. The titre of concentrated virus was directly estimated on primary neuronal cultures through visualization of eGFP four days post-infection.

Primary cortical neuron cultures were prepared from gestational day 15–16 fetuses of CD-1 mice (Charles River). Cortices were dissected and the cells dissociated by trituration in modified Eagle's medium (MEM), horse serum (20%), glucose (25 mM) and L-glutamine (2 mM) following a 15-min digestion in TrypLE (Invitrogen). The cells were plated on 6-well plates coated with poly-L-ornithine and were maintained in MEM, horse serum (10%), glucose (25 mM),

and L-glutamine (2 mM) at 37°C in a 7% CO_2 humidified incubator. The glial cell growth was inhibited by addition of 5-fluoro-2′-deoxyuridine (5F2DU, 30 μM; Sigma) to the culture medium on DI 4. The growth medium was refreshed once every third day. At DIV6, concentrated lentivirus were directly added at a multiplicity of infection of 0.5, 1 or 2 as determined through exposure in control cultures and corresponding visualization of eGFP-positive cells. At DIV10, cells were harvested into ice-cold PBS containing 1% Triton-X-100 and complete protease cocktail inhibitors (Roche).

Statistical analysis. Statistical analysis was performed with PRISM software (GraphPad Software) by using either the t-test Student or Newmann-Keuls multiple comparison tests for one-way analysis of variance.

24. Von Coelln, R. *et al.* Loss of locus coeruleus neurons and reduced startle in parkin null mice. *Proc. Natl Acad. Sci. USA* **101,** 10744–10749 (2004).
25. Alves da Costa, C., Ancolio, K. & Checler, F. Wild-type but not Parkinson's disease-related Ala53Thr-α-synuclein protect neuronal cells from apoptotic stimuli. *J. Biol. Chem* **275,** 24065–24069 (2000).
26. Qin, C. *et al.* Estrogen up-regulation of p53 gene expression in MCF-7 breast cancer cells is mediated by calmodulin kinase IV-dependent activation of a nuclear factor kappaB/CCAAT-binding transcription factor-1 complex. *Mol. Endocrinol.* **16,** 1793–1809 (2002).
27. Chung, K. K. *et al.* Parkin ubiquitinates the alpha-synuclein-interacting protein, synphilin-1: implications for Lewy-body formation in Parkinson disease. *Nature Med.* **7,** 1144–1150 (2001).
28. Alves da Costa, C. *et al.* Presenilin-dependent gamma-secretase-mediated control of p53-associated cell death in Alzheimer's disease. *J. Neurosci.* **26,** 6377–6385 (2006).
29. Goldberg, M. S. *et al.* Parkin-deficient mice exhibit nigrostriatal deficits but not loss of dopaminergic neurons. *J. Biol. Chem.* **278,** 43628–43635 (2003).
30. Abmayr, S. M., Yao, T., Parmely, T. & Workman, J. L. Preparation of nuclear and cytoplasmic extracts from mammalian cells. Curr. Protoc. Mol. Biol. **Ch 12,** Unit 12.1 (2006).
31. Coleman, J. E. *et al.* Efficient large-scale production and concentration of HIV-1-based lentiviral vectors for use *in vivo*. *Physiol. Genomics* **12,** 221–228 (2003).

nature cell biology

DOI: 10.1038/ncb1981

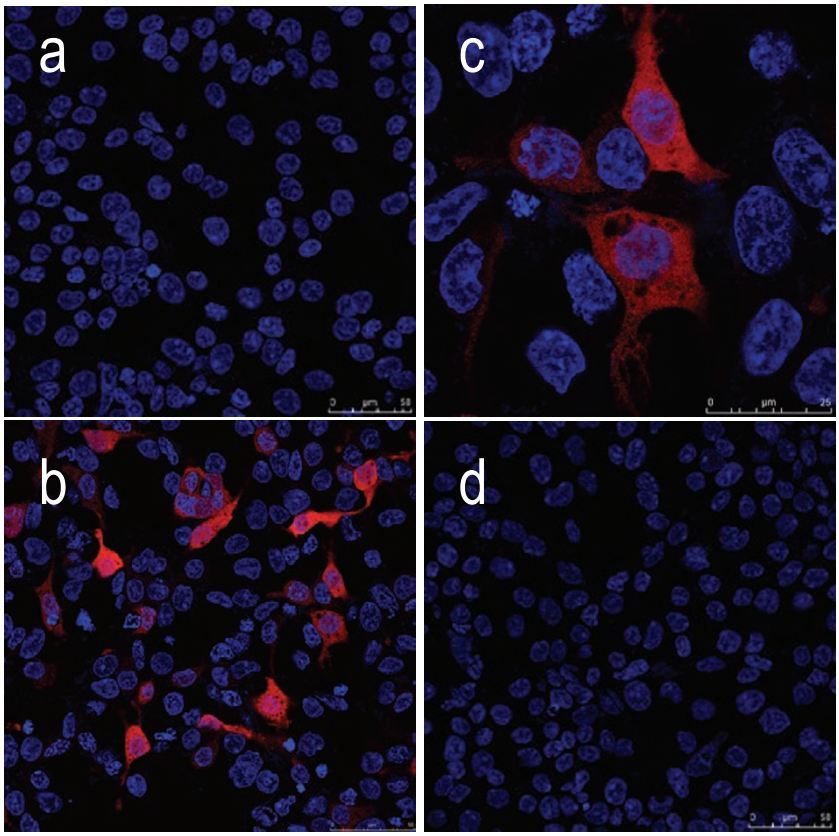

Figure S1 Parkin partitions between cytosolic and nuclear compartments. Cytosolic and nuclear localizations of parkin. HEK293 cells were transfected with either 2μg of empty vector (a) or HA-tagged Wt-Pk cDNA (b) as described in Methods and immunolabelled with anti-HA parkin antibodies (red label) or counterstained with DAPI (blue label) in order to visualize the nuclei. Confocal analysis of the images indicates a punctate label of parkin in the nuclei. Panel c represents a 2-fold amplification of the field presented in (b). Panel d represents a control where cells were incubated with the secondary antibody only.

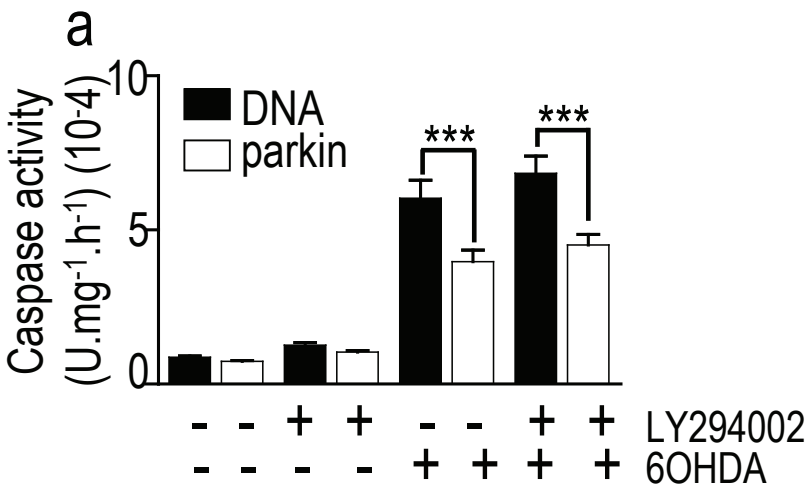

Figure S2 LY294002 does not affect parkin-associated reduction of 6OHDA-induced caspase-3 activation. SH-SY5Y neuroblastoma cells were transiently transfected with wild-type parkin (Parkin) cDNA or empty vector (DNA). Twenty-four hours after transfection, cells were pre-treated without (-) or with (+) LY294002 (10μM, 30 min) then incubated with 6OHDA (0.2mM, 8 hours). Caspase-3 activity was measured as described in the "Experimental Procedure" the means ± S.E.M of 3 independent experiments performed in duplicates. ***p<0.001. ns, not statistically significant.

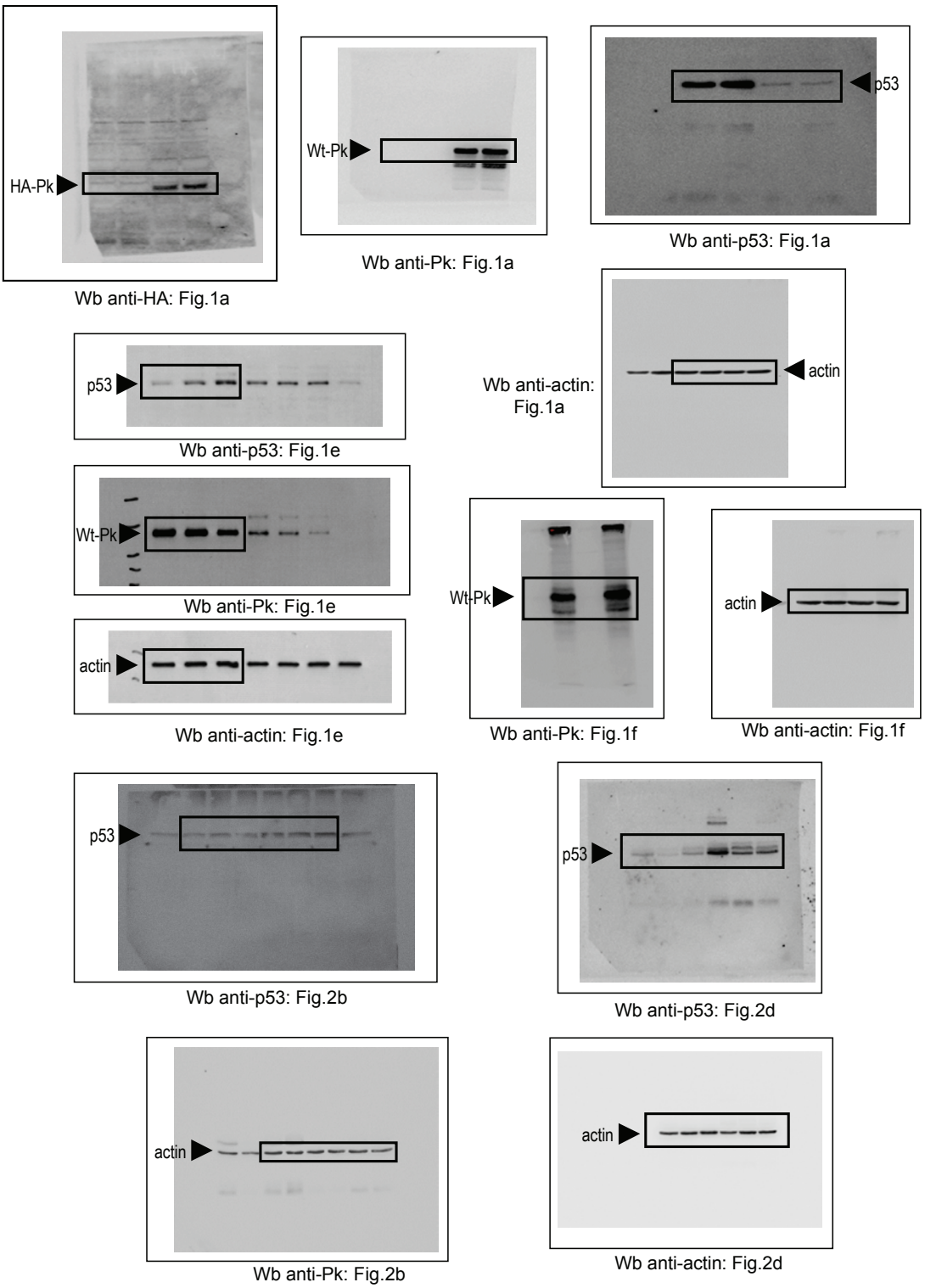

Figure S3 Full scans of western blots shown in Figs. 1a, 1e, 1f, 2b, 2d, 3b, 3d, 3g, 4d, 4e, 4f.

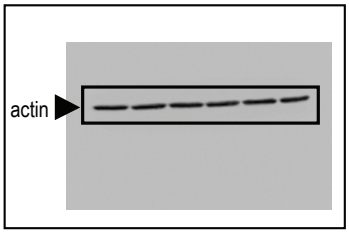

Wb anti-actin: Fig.3b

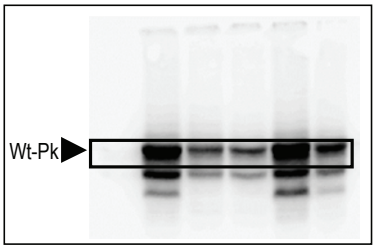

Wb anti-Pk: Fig.3b

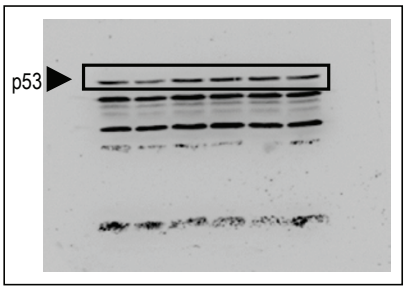

Wb anti-p53: Fig.3b

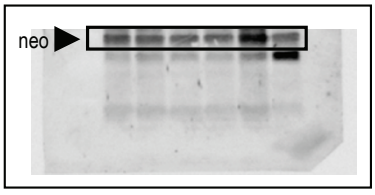

Wb anti-neomycin: Fig.3b

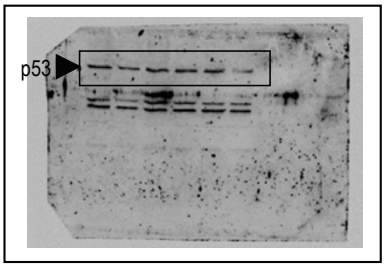

Wb anti-p53: Fig.3d

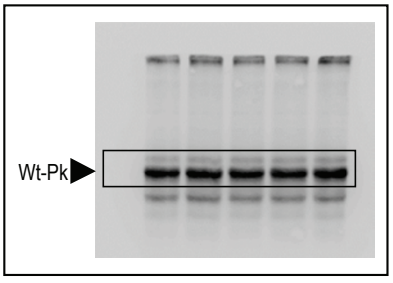

Wb anti-Pk: Fig.3d

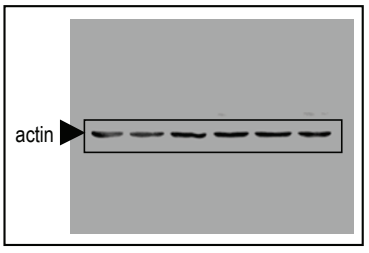

Wb anti-actin: Fig.3d

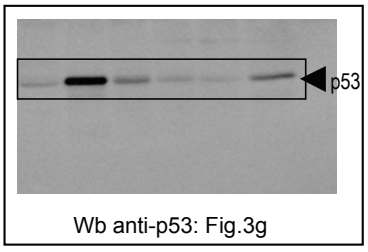

Wb anti-p53: Fig.3g

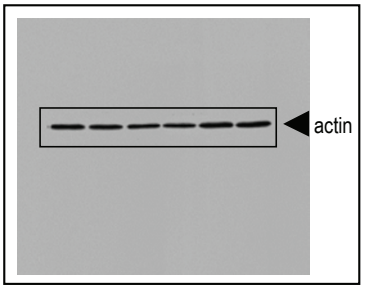

Wb anti-actin: Fig.3g

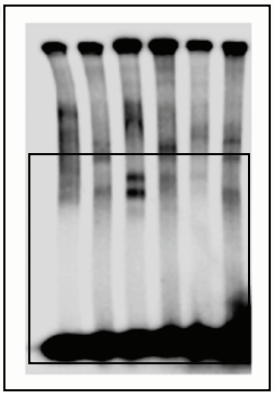

Fig.4d, left panel

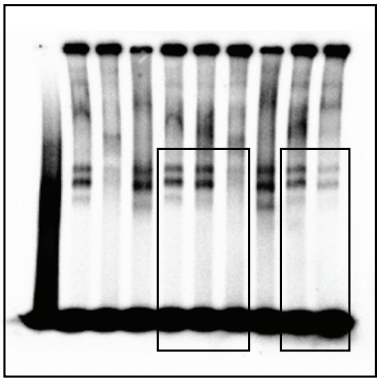

Fig.4d, right panel

Figure S3 continued

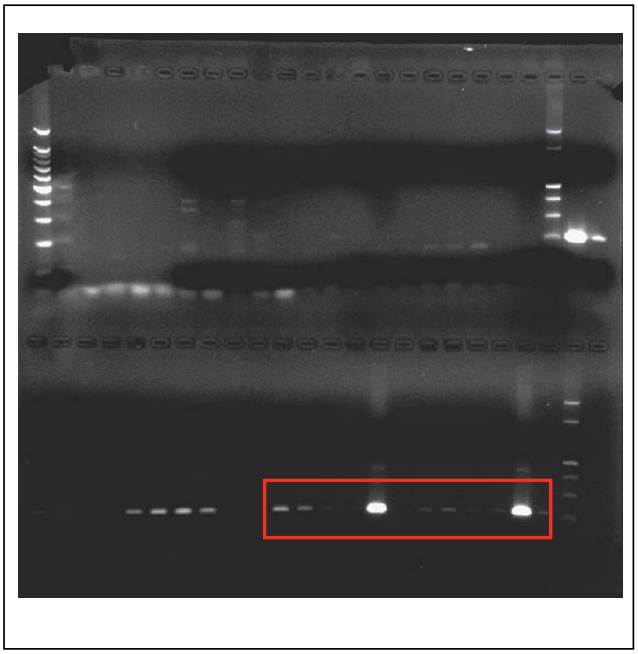

Fig.4e

Fig.4f, upper panel

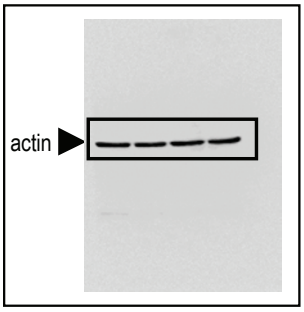

Wb anti-actin:
Fig.4f, lower panel

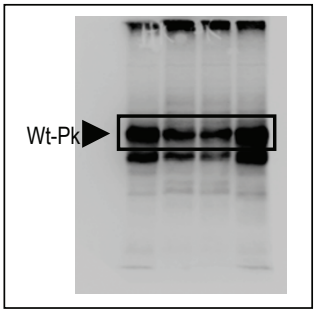

Wb anti-Pk:
Fig.4f, lower panel

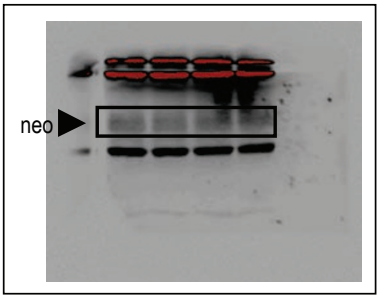

Wb anti-neomycin:
Fig.4f, lower panel

Figure S3 continued

Supplementary Table 1 Parkin mutations summary of the genetic data
For each mutation the localization within parkin domains is indicated. RING, really interesting new gene; IBR, in between ring; HTZ, heterozygous; HMZ, homozygous. The references concern their first description, but for review of all bibliographical data concerning these mutations see[1]. The R275W and exon 4 deletion variants concern the human brain material described in Methods.

Mutation	domain	type	reference
K161N	SH2-like	HTZ	Abbas et al[1]
R256C	R1	HMZ	Abbas et al[1]
C418R	R2	HTZ	Bertoli-Avella et al.[2]
C441R	R2	HTZ	West et al[3]
R275W	R1	HTZ	Unpublished
Exon 4 deletion	-	HMZ	Hayashi et al[4]

Supplemental references

1. Hampe, C., Ardila-Osorio, H., Fournier, M., Brice, A. & Corti, O. Biochemical analysis of Parkinson's disease-causing variants of Parkin, an E3 ubiquitin-protein ligase with monoubiquitylation capacity. *Hum Mol Genet* **15**, 2059-2075 (2006).
2. Abbas, N., *et al.* A wide variety of mutations in the parkin gene are responsible for autosomal recessive parkinsonism in Europe. French Parkinson's Disease Genetics Study Group and the European Consortium on Genetic Susceptibility in Parkinson's Disease. *Hum Mol Genet* **8**, 567-574 (1999).
3. Bertoli-Avella, A.M., *et al.* Novel parkin mutations detected in patients with early-onset Parkinson's disease. *Mov Disord* (2004).
4. West, A., *et al.* Complex relationship between Parkin mutations and Parkinson disease. *Am J Med Genet* **114**, 584-591 (2002).
5. Hayashi, S., *et al.* An autopsy case of autosomal-recessive juvenile parkinsonism with a homozygous exon 4 deletion in the parkin gene. *Mov Disord* **15**, 884-888 (2000).